



Published in final edited form as:

Hum Mutat. 2022 July ; 43(7): 869–876. doi:10.1002/humu.24372.

Pathogenic missense variants altering codon 336 of *GARS1* lead to divergent dominant phenotypes

Alayne P. Meyer^{1,2}, Megan E. Forrest³, Stefan Nicolau⁴, Wojciech Wiszniewski⁵, Mary Pat Bland⁵, Chang-Yong Tsao^{2,6,7}, Anthony Antonellis^{3,8}, Nicolas J. Abreu^{2,4,6}

¹Division of Genetic and Genomic Medicine, Nationwide Children's Hospital, Columbus, Ohio, USA

²Department of Pediatrics, The Ohio State University College of Medicine, Columbus, Ohio, USA

³Department of Human Genetics, University of Michigan School of Medicine, Ann Arbor, Michigan, USA

⁴The Center for Gene Therapy, Abigail Wexner Research Institute at Nationwide Children's Hospital, Columbus, Ohio, USA

⁵Department of Molecular and Medical Genetics, Oregon Health and Science University, Portland, Oregon, USA

⁶Division of Child Neurology, Nationwide Children's Hospital, Columbus, Ohio, USA

⁷Department of Neurology, The Ohio State University College of Medicine, Columbus, Ohio, USA

⁸Department of Neurology, University of Michigan School of Medicine, Ann Arbor, Michigan, USA

Abstract

Heterozygosity for missense variants and small in-frame deletions in *GARS1* has been reported in patients with a range of genetic neuropathies including Charcot–Marie–Tooth disease type 2D (CMT2D), distal hereditary motor neuropathy type V (dHMN-V), and infantile spinal muscular atrophy (iSMA). We identified two unrelated patients who are each heterozygous for a previously unreported missense variant modifying amino-acid position 336 in the catalytic domain of GARS1. One patient was a 20-year-old woman with iSMA, and the second was a 41-year-old man with CMT2D. Functional studies using yeast complementation assays support a loss-of-function effect for both variants; however, this did not reveal variable effects that might explain the phenotypic differences. These cases expand the mutational spectrum of *GARS1*-related disorders and demonstrate phenotypic variability based on the specific substitution at a single residue.

Correspondence Alayne P. Meyer, 700 Children's Dr, Columbus, OH 43205, USA. alayne.meyer@nationwidechildrens.org.
Present address

Nicolas J. Abreu, Department of Neurology, NYU Grossman School of Medicine, New York, NY, USA.

Alayne P. Meyer and Megan E. Forrest contributed equally to this study.

CONFLICTS OF INTEREST

The authors declare no conflicts of interest.

SUPPORTING INFORMATION

Additional supporting information can be found online in the Supporting Information section at the end of this article.

Keywords

Charcot–Marie–Tooth disease; complementation assay; *GARS1*; missense variant; spinal muscular atrophy

GARS1 encodes glycyl-tRNA synthetase, which catalyzes the esterification of glycine to its cognate tRNA. Several variants in the gene have been associated with either loss- or gain-of-function effects; the former affecting *GARS* localization and tRNA charging (Antonellis et al., 2006; Grice et al., 2015; Griffin et al., 2014), and the latter affecting interactions with other proteins such as neuropilin-1 (NRP1; He et al., 2015) or initiating the integrated stress response via increased binding to tRNA (Mendonça et al., 2021; Spaulding et al., 2021). While *GARS1* is ubiquitously expressed, the associated disorders primarily form a spectrum of genetic axonopathies including Charcot–Marie–Tooth disease type 2D (CMT2D), distal hereditary motor neuropathy type V (dHMN-V), and non-5q infantile spinal muscular atrophy (iSMA; Antonellis et al., 2003; James et al., 2006). *GARS1*-related CMT2D and dHMN-V were first described in 2003 and often share initial symptoms of hand weakness and atrophy with onset in childhood or early adulthood. Distal lower limb weakness may also develop in a subset of patients (Antonellis et al., 2003; Forrester et al., 2020; Markovitz et al., 2020; Yalcouyé et al., 2019). The two conditions are differentiated by the presence of sensory disturbances in CMT2D (Antonellis et al., 2003; Chung et al., 2018; Del Bo et al., 2006; Forrester et al., 2020; Markovitz et al., 2020). iSMA due to *GARS1* variants was initially described in 2006, and since then, 10 additional patients have been reported (Chung et al., 2018; Eskuri et al., 2012; Forrester et al., 2020; James et al., 2006; Liao et al., 2015; Markovitz et al., 2020). This more severe phenotype presents with symptoms beginning in the first 12 months of life and is generally associated with early respiratory failure and severe dysphagia (Chung et al., 2018; Forrester et al., 2020; Markovitz et al., 2020). The iSMA phenotype arises from variants in the anticodon binding and catalytic domains of the gene, but patients carrying other variants in these domains may also present with milder phenotypes (Chung et al., 2018; Eskuri et al., 2012; Forrester et al., 2020; James et al., 2006; Kawakami et al., 2014; H. J. Lee et al., 2012; Liao et al., 2015; Markovitz et al., 2020). Here we describe two previously unreported *GARS1* variants affecting the p.Pro336 residue, resulting in iSMA in one patient and childhood-onset CMT2D in the second. Both patients provided informed consent for participation.

Patient 1 is a 20-year-old African American female born at term following an uncomplicated pregnancy and delivery. She had no family history of neuromuscular disease. In the first months of life, she had poor feeding, a weak cry, decreased spontaneous movement, and poor head control. She developed respiratory failure requiring tracheostomy at 5.5 months and has required continuous ventilation since that time. She also had dysphagia requiring gastrostomy. She never sat unsupported, rolled, or reached for objects. She underwent surgical correction of ankle contractures and scoliosis at 3 and 14 years, respectively. She had trace antigavity elbow flexion movements as a toddler but never attained a full range of motion.

Serial examinations demonstrated the progressive weakness of the face, trunk, and extremities, which was more pronounced distally and in the lower extremities. At 20 years of age, she had bilateral facial weakness, tongue fasciculations, diffuse atrophy, areflexia, contractures, and severe weakness of the extremities, limited to trace shoulder abduction, finger flexion, and head rotation (Figure 1a). There was no movement detected in the lower extremities. She had sensory loss to large fiber modalities (i.e., vibration, proprioception) in a stocking distribution. Her cognition was unaffected.

She underwent muscle and sural nerve biopsies at 5 months of age, and again at 2 years and 8 months of age. Sural nerve pathology showed axonal degeneration (Figure 1d, e), while muscle pathology revealed denervation (Figure 1f). Electrodiagnostic studies at 5 years of age showed a severe axonal neuropathy with absent motor responses in the distal upper and lower extremities, and absent sensory responses in the lower extremities. An 83-gene next-generation sequencing panel for inherited neuropathies (including genes associated with Charcot–Marie–Tooth disease, hereditary motor neuropathy, and hereditary sensory and autonomic neuropathies) identified a de novo missense variant in *GARS1*: c.1007C > G (p.Pro336Arg). No additional variants were identified on this testing.

Patient 2 is a 41-year-old male of European ancestry. As a child, he was noted to have pes planus and to run more slowly than his peers. At age 10, he developed finger extension weakness and intrinsic hand muscle atrophy. He required multiple tendon transfers in his hands between the ages of 13–25 due to progressive weakness. He developed lower extremity symptoms including foot drop, worsening pes planus, and distal muscle atrophy, requiring ankle-foot orthotics starting at age 13. Respiratory involvement and dysphagia were absent.

Neurological examination of Patient 2 demonstrated asymmetric distal upper extremity weakness and symmetric distal lower extremity weakness (Figure 1b, c). There was no facial weakness. Deep tendon reflexes were reduced proximally and absent distally. Mild distal sensory loss was present. He was noted to have a mild tremor and a steppage gait. Electrodiagnostic studies performed at ages 19 and 27 revealed a motor axonal neuropathy or neuronopathy with minimal sensory abnormalities. The patient's family history was significant for neuropathy in his sister, brother, mother, and niece. The onset of disease was by 10 years of age in his sister, brother, and niece, while his mother had symptom onset in her early forties. A 24-gene next-generation sequencing panel for distal hereditary motor neuropathies identified a missense variant in the *GARS1* gene: c.1007C > A (p.Pro336His). This variant was present in all affected family members and absent in the patient's unaffected father. No additional variants were identified on this testing.

Patients 1 and 2 both harbor variants affecting *GARS1* p.Pro336, which is located within a stretch of highly conserved residues (including between humans and bacteria) in the catalytic domain of the protein (Figure 1g). Previous studies have shown that human *GARS1* is sufficient to rescue deletion of the yeast glycyl-tRNA synthetase ortholog *GRS1* using yeast complementation assays, and this system has been used to characterize other pathogenic, loss-of-function variants in *GARS1* (D. C. Lee et al., 2019; Opreescu et al., 2017). We therefore used this system to assess the functional impact of the p.Pro336His and

p.Pro336Arg variants. In these assays, the empty pYY1 vector was not sufficient to support yeast growth, indicating that *GRS1* is essential for yeast survival. Yeast cells transformed with wild-type *GARS1* showed appreciable growth at 30°C, indicating that expression of human *GARS1* complements deletion of yeast *GRS1* (Figure 1h). In contrast, neither p.Pro336His nor p.Pro336Arg *GARS1* supported yeast growth at 30°C, suggesting that p.Pro336His and p.Pro336Arg represent loss-of-function alleles.

To further demonstrate the impact of the p.Pro336His and p.Pro336Arg variants in the context of the previously defined GARS1 protein structure, we performed single amino-acid mutagenesis in a 3D structural model of GARS1 complexed with tRNA-Gly using PyMOL (The PyMOL Molecular Graphics System, Schrödinger, LLC). Importantly, the two GARS1 residues immediately flanking the p.Pro336 residue (p.Ser335 and p.Arg337) are known to be important for recognition of the tRNA-Gly acceptor stem by forming direct contacts with Guanine 1 and Cytosine 72 (Figure 1i; reported as p.Ser281 and p.Arg283, respectively, in the original text; Qin et al., 2014). Mutagenesis of p.Pro336 to histidine or arginine in silico (Figure 1j, k) demonstrated extensive steric clashing with surrounding residues, suggesting that these variants are likely disruptive to the overall conformation of the GARS1 catalytic domain and potentially disruptive to tRNA-Gly substrate recognition.

Patient 1 represents the 12th individual reported with infantile onset disease due to variants in *GARS1* (Table 1). All patients reported to date had variants in the catalytic ($n = 8$) or anticodon binding ($n = 4$) domains, which were de novo ($n = 8$) or inherited from an asymptomatic mosaic parent ($n = 3$). To the best of our knowledge, Patient 1 is also the oldest reported patient with infantile-onset disease, demonstrating that patients with *GARS1*-related iSMA can live into adulthood with supportive care. Even among people with *GARS1*-related iSMA, there exists significant variability in disease severity. Age of onset generally correlated with motor function and respiratory involvement. Five of six children presenting before 6 months of age required mechanical ventilation and either lost or never acquired independent sitting. By contrast, most individuals presenting at 6 months of age or older achieved and maintained independent sitting. Three could ambulate with a walker. Severe respiratory involvement can nonetheless occur in later-onset patients as well, as illustrated by two children who presented at 7 and 10 months of age and required ventilatory support. The phenotype of *GARS1*-related iSMA can be distinguished from *SMN1*-related SMA by preferential involvement of distal rather than proximal muscles, as well as the greater frequency of respiratory involvement during infancy in patients who achieve independent sitting. Other commonly reported symptoms among patients with *GARS1*-related iSMA included hypophonia, lordosis, scoliosis, ankle contractures, fasciculations, distal hyperlaxity, vocal cord dysfunction, and facial weakness. Sensory impairment was noted clinically in three and electrodiagnostically in five individuals, although many were too young for this to be assessed clinically. Electromyography in nearly all patients showed a motor axonal neuropathy or neuronopathy with variable degrees of sensory involvement. Muscle pathology in most patients was consistent with neurogenic atrophy.

Our data revealed two different *GARS1* variants affecting the same amino-acid residue that resulted in distinct phenotypes. While the cause for this discordance remains unclear,

this sensitivity to specific amino-acid substitutions has previously been described at three other residues in GARS1. The iSMA patient reported by Liao et al. (p.Asp200Tyr; Table 1) had the same residue altered as several members of a Korean family with adolescent-onset dHMN (p.Asp200Asn; H. J. Lee et al., 2012). Three siblings with iSMA reported by Chung et al. (p.Leu272Arg; Table 1) had the same amino-acid position altered as a patient with childhood-onset CMT2D who developed facial weakness and involvement of bulbar and respiratory muscles in her thirties (p.Leu272Gln, reported as p.Leu218Gln in the original text; Kawakami et al., 2014). Finally, two unrelated patients with iSMA reported by Markovitz et al. (p.Ile334Asn; Table 1) carried a variant affecting the same p.Ile334 residue as seen reported in a family with adolescent-onset dHMN-V (p.Ile334Phe, reported as p.Ile280Phe in the original text for Family 3; James et al., 2006).

These clinical differences raise questions about the underlying molecular mechanism of each mutation. For missense variants that affect the same codon, differential effects on protein function are sometimes explained by the degree of biochemical differences between the wild-type and mutant amino-acids (de Beer et al., 2013; Markovitz et al., 2020; Vitkup et al., 2003). In the present report, both variants resulted in changes to sterically large, positively charged amino acids (histidine or arginine) in place of the nonpolar proline residue resulting in clashing with other nearby amino-acid residues (Figure 1j, k), and both variants were associated with loss-of-function effects in a yeast model of GARS1 function (Figure 1h). The observed phenotypic differences may be explained in part by the degree of disruption of the original nonpolar proline residue, where substitution of the more highly charged arginine residue was associated with a more severe iSMA phenotype versus the CMT2D phenotype associated with substitution of a less basic histidine residue. While the *in vivo* and *in silico* functional studies presented here were not sufficient to differentiate the effects of these two amino-acid substitutions, careful analysis of tRNA-Gly substrate binding kinetics by more quantitative tRNA binding assays (e.g., electrophoretic mobility shift assays with labeled tRNA-Gly) could provide an explanation for differences in the observed phenotypes associated with these variants.

It is also important to consider the effects of the two different missense variants reported here in the context of proposed molecular mechanisms underlying aminoacyl-tRNA synthetase-related peripheral neuropathy. First, a dominant-negative mechanism has been proposed for loss-of-function missense alleles in cytoplasmic homodimeric aminoacyl-tRNA synthetases (Meyer-Schuman & Antonellis, 2017). Here, different amino-acid substitutions at the same residue could result in differing degrees of suppression of the wild-type protein (e.g., variable affinity for the wild-type protein). Second, GARS1 functions in the cytoplasm and mitochondria, and the different amino-acid substitutions may differentially affect mitochondrial import and/or tRNA charging in this organelle. Third, gain-of-function mechanisms have been proposed, which involve aberrant interactions between mutant GARS1 and other proteins (e.g., NRP1; He et al., 2015) or between mutant GARS1 and cognate tRNA molecules (Mendonsa et al., 2021; Spaulding et al., 2021). Therefore, different amino-acid substitutions at the same residue could result in different affinities for these proteins or tRNAs. Regarding the latter interactions, it has been proposed that increased tRNA binding results in activation of the integrated stress response (Spaulding et al., 2021), with neurons being more susceptible to the downstream effects of this

pathway. Finally, phenotypic differences could be explained by additional variants in other unidentified loci that could serve to modify GARS1 function, therefore modifying the effects of the observed disease-causing gene mutations on downstream biochemical pathways.

In summary, we have identified two previously unreported disease-causing variants that alter the same amino-acid residue (p.Pro336His and p.Pro336Arg) in *GARS1* and provided in vivo and in silico evidence of their deleterious effect on GARS1 function. The two variants led to distinct neuropathic phenotypes ranging from iSMA to CMT2D, but further work is needed to clarify the molecular mechanisms underlying these phenotypic differences.

Supplementary Material

Refer to Web version on PubMed Central for supplementary material.

ACKNOWLEDGMENTS

The authors are grateful to the affected individuals and their families for participating in this study. We would also like to thank Chin-I Chien and Chien-Chia Wang (National Central University, Taiwan) for the pYY1 expression construct. A.A. is supported by a grant from the National Institute of General Medical Sciences (GM136441). M.E.F. is supported by a Neurology Training Grant from the National Institutes of Health (5T32NS007222-40).

DATA AVAILABILITY STATEMENT

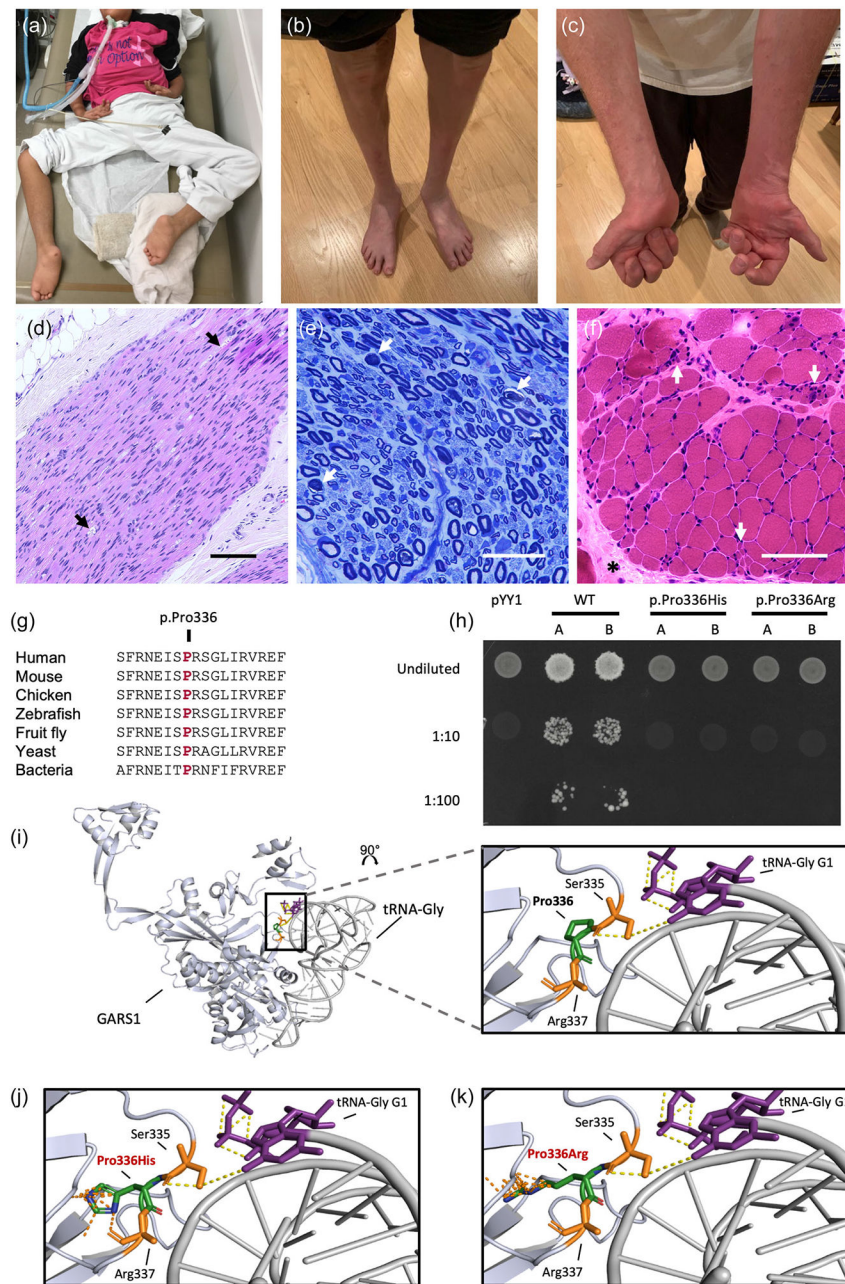
Additional clinical data or findings are available from the authors upon reasonable request. The GARS1 p.Pro336Arg variant has been submitted to ClinVar, accession number VCV001067545.2 (<https://www.ncbi.nlm.nih.gov/clinvar/>). The GARS1 p.Pro336His has been submitted to ClinVar, submission identification number SUB11111758 (<https://www.ncbi.nlm.nih.gov/clinvar/>).

REFERENCES

- Antonellis A, Ellsworth RE, Sambuughin N, Puls I, Abel A, Lee-Lin SQ, Jordanova A, Kremensky I, Christodoulou K, Middleton LT, Sivakumar K, Ionasescu V, Funalot B, Vance JM, Goldfarb LG, Fischbeck KH, & Green ED (2003). Glycyl tRNA synthetase mutations in Charcot-Marie-Tooth disease type 2D and distal spinal muscular atrophy type V. *American Journal of Human Genetics*, 72(5), 1293–1299. 10.1086/375039 [PubMed: 12690580]
- Antonellis A, Lee-Lin SQ, Wasterlain A, Leo P, Quezado M, Goldfarb LG, Myung K, Burgess S, Fischbeck KH, & Green ED (2006). Functional analyses of glycyl-tRNA synthetase mutations suggest a key role for tRNA-charging enzymes in peripheral axons. *Journal of Neuroscience*, 26(41), 10397–10406. 10.1523/JNEUROSCI.1671-06.2006 [PubMed: 17035524]
- Chung P, Northrup H, Azmath M, Mosquera RA, Moody S, & Yadav A (2018). Glycyl tRNA synthetase (GARS) gene variant causes distal hereditary motor neuropathy V. *Case Reports in Pediatrics*, 2018, 1–4. 10.1155/2018/8516285
- de Beer TAP, Laskowski RA, Parks SL, Sipos B, Goldman N, & Thornton JM (2013). Amino acid changes in disease-associated variants differ radically from variants observed in the 1000 Genomes Project Dataset. *PLoS Computational Biology*, 9(12), e1003382. 10.1371/journal.pcbi.1003382 [PubMed: 24348229]
- Del Bo R, Locatelli F, Corti S, Scarlato M, Ghezzi S, Prella A, Fagiolari G, Moggio M, Carpo M, Bresolin N, & Comi GP (2006). Coexistence of CMT-2D and distal SMA-V phenotypes in an Italian family with a GARS gene mutation. *Neurology*, 66(5), 752–754. 10.1212/01.wnl.0000201275.18875.ac [PubMed: 16534118]

- Deng X, Qin X, Chen L, Jia Q, Zhang Y, Zhang Z, Lei D, Ren G, Zhou Z, Wang Z, Li Q, & Xie W (2016). Large conformational changes of insertion 3 in human glycyl-tRNA synthetase (hGlyRS) during catalysis. *Journal of Biological Chemistry*, 291(11), 5740–5752. 10.1074/jbc.M115.679126 [PubMed: 26797133]
- Eskuri JM, Stanley CM, Moore SA, & Mathews KD (2012). Infantile onset CMT2D/dSMA V in monozygotic twins due to a mutation in the anticodon-binding domain of GARS. *Journal of the Peripheral Nervous System*, 17(1), 132–134. 10.1111/j.1529-8027.2012.00370.x [PubMed: 22462675]
- Farwell KD, Shahmirzadi L, El-Khechen D, Powis Z, Chao EC, Tippin Davis B, Baxter RM, Zeng W, Mroske C, Parra MC, Gandomi SK, Lu I, Li X, Lu H, Lu H-M, Salvador D, Ruble D, Lao M, Fischbach S, ... Tang S (2015). Enhanced utility of family-centered diagnostic exome sequencing with Inheritance model-based analysis: Results from 500 unselected families with undiagnosed genetic conditions. *Genetics in Medicine*, 17(7), 578–586. 10.1038/gim.2014.154 [PubMed: 25356970]
- Forrester N, Rattihalli R, Horvath R, Maggi L, Manzur A, Fuller G, Gutowski N, Rankin J, Dick D, Buxton C, Greenslade M, & Majumdar A (2020). Clinical and genetic features in a series of eight unrelated patients with neuropathy due to glycyl-tRNA synthetase (GARS) variants. *Journal of Neuromuscular Diseases*, 7(2), 137–143. 10.3233/JND-200472 [PubMed: 31985473]
- Grice SJ, Sleight JN, Motley WW, Liu JL, Burgess RW, Talbot K, & Cader MZ (2015). Dominant, toxic gain-of-function mutations in gars lead to non-cell autonomous neuropathology. *Human Molecular Genetics*, 24(15), 4397–4406. 10.1093/hmg/ddv176 [PubMed: 25972375]
- Griffin LB, Sakaguchi R, Mcguigan D, Gonzalez MA, Searby C, Züchner S, Hou YM, & Antonellis A (2014). Impaired function is a common feature of neuropathy-associated glycyl-tRNA synthetase mutations. *Human Mutation*, 35(11), 1363–1371. 10.1002/humu.22681 [PubMed: 25168514]
- He W, Bai G, Zhou H, Wei N, White NM, Lauer J, Liu H, Shi Y, Dumitru CD, Lettieri K, Shubayev V, Jordanova A, Guergueltcheva V, Griffin PR, Burgess RW, Pfaff SL, & Yang XL (2015). CMT2D neuropathy is linked to the neomorphic binding activity of glycyl-tRNA synthetase. *Nature*, 526(7575), 710–714. 10.1038/nature15510 [PubMed: 26503042]
- James PA, Cader MZ, Muntoni F, Childs AM, Crow YJ, & Talbot K (2006). Severe childhood SMA and axonal CMT due to anticodon binding domain mutations in the GARS gene. *Neurology*, 67(9), 1710–1712. 10.1212/01.wnl.0000242619.52335.bc [PubMed: 17101916]
- Kawakami N, Komatsu K, Yamashita H, Uemura K, Oka N, Takashima H, & Takahashi R (2014). A novel mutation in glycyl-tRNA synthetase caused Charcot–Marie–Tooth disease type 2D with facial and respiratory muscle involvement. *Clinical Neurology*, 54(11), 911–915. 10.5692/clinicalneuro.54.911 [PubMed: 25420567]
- Lee DC, Meyer-Schuman R, Bacon C, Shy ME, Antonellis A, & Scherer SS (2019). A recurrent GARS mutation causes distal hereditary motor neuropathy. *Journal of the Peripheral Nervous System*, 24(4), 320–323. 10.1111/jns.12353 [PubMed: 31628756]
- Lee HJ, Park J, Nakhro K, Park JM, Hur YM, Choi BO, & Chung KW (2012). Two novel mutations of GARS in Korean families with distal hereditary motor neuropathy type v. *Journal of the Peripheral Nervous System*, 17(4), 418–421. 10.1111/j.1529-8027.2012.00442.x [PubMed: 23279345]
- Liao YC, Liu YT, Tsai PC, Chang CC, Huang YH, Soong BW, & Lee YC (2015). Two novel de novo GARS mutations cause early-onset axonal Charcot–Marie–Tooth disease. *PLoS ONE*, 10(8), e0133423. 10.1371/journal.pone.0133423 [PubMed: 26244500]
- Markovitz R, Ghosh R, Kuo ME, Hong W, Lim J, Bernes S, Manberg S, Crosby K, Tanpaiboon P, Bharucha-Goebel D, Bonnemann C, Mohila CA, Mizerik E, Woodbury S, Bi W, Lotze T, Antonellis A, Xiao R, & Potocki L (2020). GARS-related disease in infantile spinal muscular atrophy: Implications for diagnosis and treatment. *American Journal of Medical Genetics, Part A*, 182(5), 1167–1176. 10.1002/ajmg.a.61544 [PubMed: 32181591]
- Mendonça S, von Kuegelgen N, Bujanic L, & Chekulaeva M (2021). Charcot–Marie–Tooth mutation in glycyl-tRNA synthetase stalls ribosomes in a pre-accommodation state and activates integrated stress response. *Nucleic Acids Research*, 49(17), 10007–10017. 10.1093/nar/gkab730 [PubMed: 34403468]

- Meyer-Schuman R, & Antonellis A (2017). Emerging mechanisms of aminoacyl-tRNA synthetase mutations in recessive and dominant human disease. *Human Molecular Genetics*, 26(R2), R114–R127. 10.1093/hmg/ddx231 [PubMed: 28633377]
- Opreacu SN, Chepa-Lotrea X, Takase R, Golas G, Markello TC, Adams DR, Toro C, Gropman AL, Hou YM, Malicdan MCV, Gahl WA, Tift CJ, & Antonellis A (2017). Compound heterozygosity for loss-of-function GARS variants results in a multisystem developmental syndrome that includes severe growth retardation. *Human Mutation*, 38(10), 1412–1420. 10.1002/humu.23287 [PubMed: 28675565]
- Qin X, Hao Z, Tian Q, Zhang Z, Zhou C, & Xie W (2014). Cocrystal structures of glycyl-tRNA synthetase in complex with tRNA suggest multiple conformational states in glycylation. *Journal of Biological Chemistry*, 289(29), 20359–20369. 10.1074/jbc.M114.557249 [PubMed: 24898252]
- Spaulding EL, Hines TJ, Bais P, Tadenev A, Schneider R, Jewett D, Pattavina B, Pratt SL, Morelli KH, Stum MG, Hill DP, Gobet C, Pipis M, Reilly MM, Jennings MJ, Horvath R, Bai Y, Shy ME, Alvarez-Castelao B, ... Burgess RW (2021). The integrated stress response contributes to tRNA synthetase-associated peripheral neuropathy. *Science*, 373(6559), 1156–1161. 10.1126/science.abb3414 [PubMed: 34516839]
- Vitkup D, Sander C, & Church GM (2003). The amino-acid mutational spectrum of human genetic disease. *Genome Biology*, 4(11), R72. 10.1186/gb-2003-4-11-r72 [PubMed: 14611658]
- Yalcouyé A, Diallo SH, Coulibaly T, Cissé L, Diallo S, Samassékou O, Diarra S, Coulibaly D, Keita M, Guinto CO, Fischbeck K, & Landouré G (2019). A novel mutation in the GARS gene in a Malian family with Charcot–Marie–Tooth disease. *Molecular Genetics and Genomic Medicine*, 7(7), e00782. 10.1002/mgg3.782 [PubMed: 31173493]

**FIGURE 1.**

(a) Clinical findings of Patient 1; note diffuse atrophy and distal contractures of four extremities with tracheostomy in situ requiring continuous ventilation and gastrostomy tube present (latter not shown). (b, c) Clinical findings of Patient 2; note atrophy of distal lower limb musculature and intrinsic hand muscles, with severe finger extension weakness and flexion contractures. (d, e) Sural nerve biopsy findings in Patient 1 from 5 months of age. (d) Occasional myelin digestion chambers were present (arrows). Hematoxylin and eosin stain, scale bar = 100 μ m. (e) The density of large myelinated nerve fibers was mildly reduced and scattered axons showed signs of degeneration (arrows). Toluidine blue stain, scale bar = 25 μ m. (f) Muscle biopsy performed at 2 years and 8 months of age in Patient

1 demonstrates small groups of atrophic fibers (arrows) and increased perimysial connective tissue (*). Hematoxylin and eosin stain, scale bar = 100 μ m. (g, k) Functional studies of the p.Pro336His and p.Pro336Arg *GARS1* variants. (g) The p.Pro336 amino acid is highly conserved from humans to bacteria (*T. thermophilus*). (h) Haploid yeast lacking endogenous *GRS1* were rescued by wild-type human *GARS1*, but not by p.Pro336His or p.Pro336Arg *GARS1*, nor by a vector with no *GARS1* insert (pYY1). Replicates A and B indicate yeast colonies obtained from two independent transformations. Image shown is representative of three independent transformations using three different plasmid DNA preparations. (i) (left) PyMOL model generated using a Protein Database (PDB) structural data file for GARS1 complexed with tRNA-Gly in a crystal lattice (Deng et al., 2016; PDB accession 4QEI). The model represents a monomer of GARS1 protein (light blue) complexed with a single tRNA-Gly (gray) for simplicity; note that GARS1 functions as a homodimer in vivo. (right) Enlarged and rotated view of GARS1 Pro336 (green) and surrounding residues within the GARS1 catalytic domain (Ser335 and Arg337, orange) along with the tRNA-Gly acceptor stem (G1, purple). (j, k) Enlarged and rotated views of the (j) GARS1 Pro336His and (k) Pro336Arg amino-acid substitutions modeled using PyMOL protein mutagenesis. Steric clashing with surrounding residues in neighboring areas of the GARS1 catalytic domain are indicated by orange dashed lines

TABLE 1

Summary of infantile spinal muscular atrophy patients due to *GARS1* variants (All NM_002047.2/NP_002038.2)

| Variant | Inheritance | Domain | Age of onset | Age at last examination | Highest gross motor function (age attained) | Respiratory failure (Y/N) (age started) | G-tube (Y/N) (age started) | Other reported features | EMG/NCS | Muscle biopsy | Source |
|---------------------------|--------------------|-----------|--------------|-------------------------|--|---|----------------------------|---|--|--|--|
| c.373G > A (p.Glu125Lys) | De novo | Catalytic | 3m | NR | NR | Y (7m) | Y (7m) | Distal > proximal weakness | Severe motor neuropathy/neuronopathy without sensory involvement | NR | Farwell et al. (2015), Forrester et al. (2020) |
| c.598G > T (p.Asp200Tyr) | De novo | Catalytic | 3m | 9y | Sit unsupported (15m) | N (temporarily at 3m with pneumonia) | N | Pes planus, distal > proximal weakness, sensory impairment | Severe sensorimotor neuropathy | NR | Liao et al. (2015) |
| c.815T > G (p.Leu272Arg) | Maternal mosaicism | Catalytic | 10m | 2y | Sit unsupported (24m) | Y (10m) | Y (12m) | Distal hyperlaxity | Motor axonal neuropathy/neuronopathy without sensory involvement | Denervation atrophy | Chung et al. (2018) |
| c.815T > G (p.Leu272Arg) | Maternal mosaicism | Catalytic | 7m | 7m | NR | Y (7m) | NR | Distal hyperlaxity | NR | NR | Chung et al. (2018) |
| c.815T > G (p.Leu272Arg) | Maternal mosaicism | Catalytic | 9m | 4y | Normal motor development (9m) | N | N | Distal hyperlaxity | Normal sensory function | NR | Chung et al. (2018) |
| c.1001T > A (p.Ile334Asn) | De novo | Catalytic | 2m | 11m | Less than antigravity in lower extremities (11m) | Y (3m) | Y | Oligohydramnios, fasciculations, proximal > distal weakness | Predominantly motor axonal neuropathy/neuronopathy with mild sensory involvement | Denervation atrophy | Markovitz et al. (2020) |
| c.1001T > A (p.Ile334Asn) | De novo | Catalytic | 1.5m | 3.25y | Rolled (3m, lost at 18m), sit unsupported (12m, lost at 39m) | Y (2m) | Y | Distal > proximal weakness, claw-like hands, pes cavus, ankle contractures, sensory impairment, kyphoscoliosis, mildly increased prominence of CSF spaces | Severe sensorimotor axonal neuropathy predominantly affecting motor fibers | Denervation atrophy with features of chronic active myopathy | Markovitz et al. (2020) |
| c.1007C > G (p.Pro336Arg) | De novo | Catalytic | <5m | 20y | Head control, antigravity elbow flexion | Y (5m) | Y (6m) | Scoliosis, distal > proximal weakness, facial weakness, hypophonia, fasciculations, contractures, sensory impairment, | Severe axonal sensorimotor neuropathy | Denervation atrophy | Current study |

| Variant | Inheritance | Domain | Age of onset | Age at last examination | Highest gross motor function (age attained) | Respiratory failure (Y/N) (age started) | G-tube (Y/N) (age started) | Other reported features | EMG/NCS | Muscle biopsy | Source |
|---------------------------|------------------|-------------------|--------------|-------------------------|--|---|----------------------------|---|---|---|-------------------------|
| c.1954G > C (p.Gly652Arg) | De novo | Anticodon binding | Birth | 14m | Movement of arms/legs (lost) | Y (4m) | Y | ankle contractures, dysconjugate gaze, high palate, crowded dentition, tented upper lip | Severe sensorimotor neuropathy predominantly affecting motor fibers | NR | Markovitz et al. (2020) |
| c.1955G > C (p.Gly652Ala) | Presumed de novo | Anticodon binding | 6m | 7y | Sit unsupported (6m), walk with walker (18m) | N (FVC 80%) | N | Hypophonia, facial weakness, weak cough, hyperlordosis, preserved proximal strength | EMG consistent with denervation | Denervation atrophy | James et al. (2006) |
| c.1955G > C (p.Gly652Ala) | De novo | Anticodon binding | 6m | 3.75y | Walk with walker | NR | NR | Hyperlordosis, vocal cord dysfunction, height/weight <1st% | NR | Fiber size variability and marked type I fiber predominance | Eskuri et al. (2012) |
| c.1955G > C (p.Gly652Ala) | De novo | Anticodon binding | 6m | 3.75y | Walk with walker | NR | NR | Hyperlordosis, kyphoscoliosis, vocal cord dysfunction, height/weight <1st% | Motor axonal neuropathy/neuronopathy | NR | Eskuri et al. (2012) |

Abbreviations: CSF, cerebrospinal fluid; EMG/NCS, electromyography/nerve conduction studies; FVC, forced vital capacity; m, months; N, no; NR, not reported; y, years; Y, yes.